

Design and Synthesis of ATP-Based Nucleotide Analogues and Profiling of Nucleotide-Binding Proteins

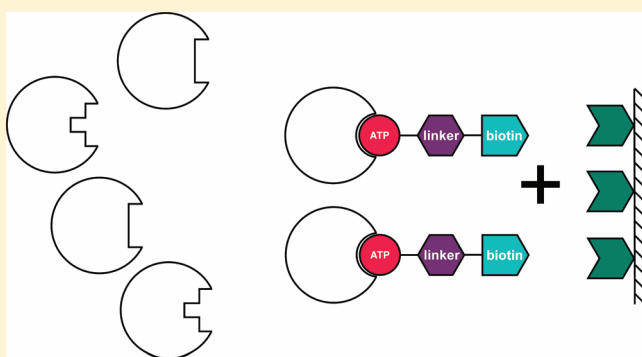
Justina. C. Wolters,[†] Gerard Roelfes,[‡] and Bert Poolman^{*,†}

[†]Department of Biochemistry, Groningen Biomolecular Sciences and Biotechnology Institute, Netherlands Proteomics Centre & Zernike Institute for Advanced Materials

[‡]Department of Biomolecular Chemistry, Stratingh Institute for Chemistry University of Groningen, Nijenborgh 4, 9747 AG Groningen, The Netherlands

S Supporting Information

ABSTRACT: Two nucleotide-based probes were designed and synthesized in order to enrich samples for specific classes of proteins by affinity-based protein profiling. We focused on the profiling of adenine nucleotide-binding proteins. Two properties were considered in the design of the probes: the bait needs to bind adenine nucleotide-binding proteins with high affinity and carry a second functional group suitable and easily accessible for coupling to a chromatography resin. For this purpose, we synthesized *p*-biotinyl amidobenzoic acid-ATP (*p*-BABA-ATP) and *p*-biotinyl aminomethylbenzoic acid-ATP (*p*-BAMBA-ATP). *p*-BABA-ATP and *p*-BAMBA-ATP both bind to ATP-binding cassette (ABC) proteins with at least 10-fold higher affinity than ATP. Several ABC transporters could be enriched using *p*-BABA-ATP or *p*-BAMBA-ATP.



INTRODUCTION

In activity-based protein profiling, protein classes are enriched via a reactive probe that requires the protein or protein domain to be functional. The probe (bait) contains a reactive group and a reporter tag, usually connected via a linker moiety. The binding moiety is designed to react with a specific class of proteins, and the reporter tag of the probe enables their detection and/or enrichment (via fluorescent, affinity, antigen, or isotope-labeled reporter tags). The use of different binding moieties and reactive groups can help in the analysis of the active site of the proteins. The probes can be used to screen for inhibitors via competitive binding studies, with the clear advantage that experiments can be performed in complex mixtures without the requirement for prior enrichment steps (e.g., as used for the identification of drug targets).¹ This protein profiling is routinely done in cell homogenates rather than *in vivo*, because the size of the probes limits their uptake and distribution in the cells. This limitation can be overcome by splitting the label into two parts: a cross-linking group and a reporter tag (fluorescent probe or biotin tag). Both parts of the probe contain an extra reactive group to attach the two halves, using so-called click chemistry (see refs 2,3,4 for click chemistry implemented in activity-based probes). Numerous reviews about activity-based proteomics and their applications have been published in recent years.^{5–11}

For the use of ATP analogues, modifications to all three moieties of ATP (the nucleobase, ribose ring, or phosphate

groups) have been prepared, yielding nucleotide analogues with different functionalities. The reporter analogues can be divided in molecules with spectroscopic or radioactive moieties and probes that can bind to antibodies or column based materials (like a biotin moiety).^{12–15} The features of ATP analogues in studies of nucleotide-binding proteins, in combination with their structures, have been exploited by us to find patterns for modifications. ATP analogues with small modifications at the nucleobase (like azido-ATP, ϵ ATP) and phosphate (AMP-PNP, AMP-PCP, and ATP γ S) of ATP are tolerated by most adenine nucleotide-binding proteins. Bulkier groups are generally restricted to either the phosphate or ribose ring. The extents to which these modifications are tolerated vary for the different classes (adenine) nucleotide-binding proteins.

Adenine nucleotide-binding proteins cover a large range of protein classes. They can use ATP as source of metabolic energy in living cells, fueling of transport (via transport ATPases) or movement (via molecular motors), and phosphorylation of enzymes and small metabolites via kinases. Most often, ATP (binding and/or hydrolysis) is used in coupling reactions and drives the endergonic steps. Moreover, it is a substrate and/or cofactor involved in DNA/RNA modifying processes like transcription, DNA

Received: January 4, 2011

Revised: April 21, 2011

Published: June 21, 2011

replication, recombination, and restriction. Besides its function as energy storage unit or substrate for the biosynthesis of DNA/RNA, ATP acts as a signaling molecule for proteins belonging to the class of purinergic receptors. The probes described in this paper were designed for screening of proteins from the ATP-binding cassette (ABC) superfamily but are likely to have broader uses.

Within the class of the adenine nucleotide-binding proteins, ABC proteins play an important role in a wide range of physiological functions, mostly involving translocation of compounds across the membrane (so-called ABC transporters).¹⁶ At least eighteen of the human ABC genes are associated to diseases, including cystic fibrosis (ABCC7), Tangier disease (ABCA1), immune deficiency (ABCB2/3), and many others (listed in ref 17 and on <http://nutrigene.4t.com/humanabc.htm>).

ABC transporters share a conserved overall architecture with two conserved nucleotide-binding domains (NBDs) and two transmembrane domains (TMDs). The transmembrane domains form a pathway through the membrane for the translocation of the substrates. The energy needed for the translocation is provided by ATP that binds to the NBDs and is hydrolyzed at these sites. A limited number of ATP analogues have been exploited to probe functional and structural aspects of ABC proteins. The fluorescent ATP analogues trinitrophenyl-ATP (TNP-ATP), but also the cross-linking azido-derivatives,¹⁸ have been used to determine binding constants for nucleotides.^{19,20} The non- (or slowly) hydrolyzable analogues AMP-PNP^{21–23} and ATP γ S^{24,25} have been used to dissect the effects of adenine nucleotide binding and hydrolysis. Profiling of ABC proteins has, to the best of our knowledge, not been reported.

Here, we describe the synthesis of two adenine nucleotide analogues, *p*-biotinyl amidobenzoic acid-ATP (*p*-BABA-ATP) and *p*-biotinyl aminomethylbenzoic acid-ATP (*p*-BAMBA-ATP), their structural characterization, and their binding to the ABC transporter OpuA. As a proof of principle for the profiling of ABC transporters, several ABC and non-ABC transporters were used for the characterization of the ATP analogues.

EXPERIMENTAL SECTION

Synthesis of Biotinylated Linkers. The synthesis of biotinylated linkers is based on a description of biotinylated amino acid precursors by Skander et al.²⁶ Briefly, biotin (2.1 mmol) was dissolved in DMF (40 mL) with tributylamine (0.64 mL, 2.7 mmol). isobutyl chloroformate (0.32 mL, 2.5 mmol) was added to the solution to activate the biotin, and the mixture was incubated at room temperature for about 15 min after which it was cooled on ice. Meanwhile, linker (4.1 mmol) was dissolved in DMF (40 mL) and cooled on ice. After cooling, the activated biotin mixture was slowly added to the linker dissolved in DMF, and the mixture was incubated for two hours at 5 °C. The solvent was removed under vacuum, the crude precipitate was recrystallized from 3:1 ethanol/H₂O, and the obtained crystals were washed extensively with water and ethanol. The reaction was performed with two different linkers: *p*-aminobenzoic acid (*p*-ABA) and *p*-aminomethylbenzoic acid (*p*-AMBA). Both biotinylated linkers recrystallized as a white solid, but the recrystallized solid of the biotinylated *p*-aminomethylbenzoic acid was more hygroscopic compared to the solid of the biotinylated *p*-aminobenzoic acid. The yield of pure biotinylated linker was about 40% and the purity of the products was analyzed by NMR:

p-Biotinyl-amidobenzoic Acid (*p*-BABA). ¹H NMR (300 MHz, CD₃SOCD₃): δ = 1.34–1.62 (m, 6H), 2.33 (t, *J* = 7.3 Hz, 2H), 2.56 (d, *J* = 12.5, 1H), 2.80 (dd, *J* = 12.5, 5.1 Hz, 1H), 3.07–3.13 (m, 1H), 4.12 (t, *J* = 5.1 Hz, 1H), 4.29 (t, *J* = 6.2 Hz, 1H), 6.39 (d, *J* = 23.4 Hz, 2H), 7.68 (d, *J* = 8.8 Hz, 2H), 7.85 (d, *J* = 8.8, 2H). ¹³C NMR (200 MHz, CD₃SOCD₃): δ = 25.1, 28.3, 36.5, 55.5, 59.4, 61.3, 118.5, 125.1, 130.5, 143.4, 163.0, 167.2, 172.1. ESI-MS: calculated mass C₁₇H₂₁N₃O₄S 363.44, found *m/z* [M][−] 362.6.

p-Biotinyl-amidobenzoic Acid (*p*-BAMBA). ¹H NMR (300 MHz, CD₃SOCD₃): δ 1.31–1.57 (m, 6H), 2.14 (t, *J* = 7.1 Hz, 2H), 2.56 (d, *J* = 12.5 Hz, 1H), 2.81 (dd, *J* = 12.5, 5.1 Hz), 3.06–3.09 (m, 1H), 4.11 (t, *J* = 5.1 Hz, 1H), 4.27–4.31 (m, 3H), 6.39 (d, *J* = 21.2 Hz, 2H), 7.33 (d, *J* = 8.4 Hz, 2H), 7.87 (d, *J* = 8.4 Hz, 2H), 8.41 (t, *J* = 5.5 Hz, 1H). ESI-MS: calculated mass C₁₈H₂₃N₃O₄S 377.47, found *m/z* [M][−] 376.2.

Synthesis Biotinyl-linker-ATP. The synthesis of the biotinyl-linker-ATP complex is adapted from the synthesis of 3'-O-(4'-benzoyl)benzoyl-ATP as described by Williams et al.²⁷ Glassware was dried at 160 °C prior to use. Biotinylated linker (0.5 mmol) was dissolved in dry DMF (3 mL) together with carbonyldiimidazole (CDI) (1.2 mmol), keeping the setup with the dried glassware under a flow of nitrogen. The reaction was monitored by the evaporation of CO₂ gas, which stopped after 1 h after addition of CDI. Then, ATP (0.5 mmol) in H₂O (12 mL) was added to the mixture, and the reaction was incubated for 6 h under constant stirring at room temperature.

The crude reaction mixture was purified in batches (5 mL) by RP-HPLC, using a preparative C18 column (prepared from Vydac218TPB_101SRPC column material; column dimensions 25/132) connected to an Äkta-purifier system. The column was run at a flow rate of 3 mL/min, using buffer A, triethylammoniumacetate (TEAA, 10 mM) pH 7, and buffer B, acetonitrile plus TEAA pH 7 (10 mM), and the following gradient: 35 min 5% buffer B, 75 min gradient 5–35% buffer B, 15 min 90% buffer B, 15 min 0% buffer B. Fifteen milliliter fractions were collected and analyzed by ESI-MS to determine the fractions containing the ATP analogue. ATP analogue peak fractions of multiple runs were pooled and freeze-dried, and the material was then resuspended in TEAA pH 7 (200 mM) and loaded onto a 1 mL monoQ sepharose column, pre-equilibrated with 20 column volumes TEAA pH 7 (200 mM). The column was washed with 2 × 10 column volumes TEAA pH 7 (200 mM) and eluted with 4 × 5 column volumes TEAA pH 7.0 (1M). Multiple rounds of freeze-drying (the solids were resuspended in Milli-Q) were done to remove the (volatile) TEAA pH 7 completely. The yield of pure product was about 20% based on the amount of the pure ATP analogues (dry weight). The final products were analyzed with ESI-MS:

p-Biotinyl-amidobenzoic Acid-ATP (*p*-BABA-ATP). (ESI-MS), calculated mass C₂₇H₃₅N₈O₁₆P₃S 852,61, found *m/z* [M][−] 851.71 (ACN (50%) plus formic acid (0.1%))/ 851.3 (methanol).

p-Biotinyl-amidobenzoic acid-ATP (*p*-BAMBA-ATP). (ESI-MS), calculated mass C₂₈H₃₇N₈O₁₆P₃S 866.64, found *m/z* [M][−] 865.6 (ACN (50%) plus formic acid (0.1%)).

Spectral Properties. UV spectra of *p*-BABA-ATP and *p*-BAMBA-ATP were measured on a Cary100 Bio UV–visible spectrophotometer (Varian) with samples of 400 μ L (20 μ M in a quartz cuvette, with maxima for *p*-BABA-ATP (264 nm), *p*-BABA (260 nm), ATP (258 nm), *p*-BAMBA-ATP (245 nm), and *p*-BAMBA (230 nm). The molar extinction coefficient was not altered upon modification of ATP, and under the experimental conditions, ATP, *p*-BABA-ATP, and *p*-BAMBA-ATP all

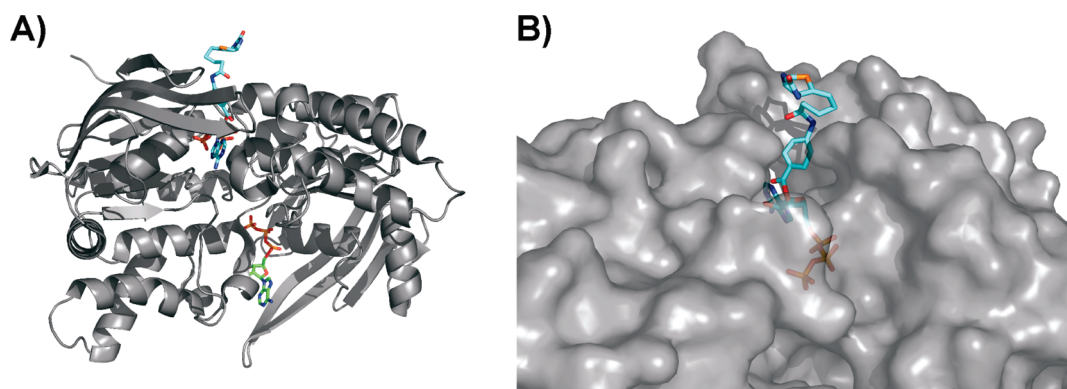


Figure 1. X-ray crystallography structure of the ATPase dimer of the ABC transporter MJ0796 (1L2T).⁴⁹ The structure was solved in the presence of ATP (panel A, ATP green/orange), showing the position of the nucleotides. One of the ATP molecules was overlaid with the ATP analogue *p*-BABA-ATP (in blue/orange). Panel B depicts an enlargement of a space-filling model of MJ0796 with the ATP analogue, showing the accessibility of the biotin group.

had molar extinction coefficients of around $15\,000\text{ M}^{-1}\text{ cm}^{-1}$ at their respective absorption maxima.

Partial Hydrolysis of *p*-BABA-ATP. A few milligrams of *p*-BABA-ATP was dissolved in methanol ($250\ \mu\text{L}$). Sodium carbonate was added until the total volume was filled about half-way with powder, to ensure saturating conditions. The mixture was incubated for 1 h at $40\ ^\circ\text{C}$, under mixing (800 rpm). The mixture was shortly spun down and the supernatant was mixed 1:1 with ACN (50%) plus formic acid (0.1%). Formic acid was added for the ESI-MS analysis. For ESI-MS/MSMS analysis, the samples were diluted $10\times$ in ACN (50%) plus formic acid (0.1%).

Analytical Methods. Nuclear magnetic resonance spectra were recorded with a 200/300 MHz (^1H NMR) or 50/75 MHz (^{13}C NMR) spectrometer. Chemical shifts are reported in delta (δ) units, parts per million (ppm), and as an average shift for split peaks. Coupling constants (J) are reported in Hz.

ESI-MS spectra were measured with a LCQ fleet mass spectrometer (Thermo scientific) via direct injection at a flow rate of $10\ \mu\text{L}/\text{min}$. Settings of the spectrometer were tuned with a standard solution of ATP both in positive and negative ion mode. Samples were diluted in ACN (50%) plus formic acid (0.1%) prior to the measurements. ESI-MS/MSMS mass spectra were recorded on an API3000 triple quadrupole mass spectrometer equipped with a TurboIonSpray source (MDS-Sciex, Concord, Ontario, Canada) in positive ion mode with nitrogen as collision gas, at a collision energy of 40 eV.

Analytical RP-HPLC was performed using a polystyrene/divenyl benzene column (Source SRPC ST 4.6/150) connected to an Äkta-purifier system. Two buffers were used for the separation: Buffer A, TEAA (100 mM) pH 7.0, and Buffer B, acetonitrile plus TEAA (100 mM) pH 7.0. The settings for the separations were as follows: $200\ \mu\text{L}$ loop, flow $1\ \text{mL}/\text{min}$, gradient: 5 min 17% buffer B, 10 min gradient 17–20% buffer B, 5 min 90% buffer B, 5 min 0% B.

TNP-ATP Binding. Purified OpuA ($0.7\ \mu\text{M}$) was preincubated for 10 min with TNP-ATP ($2\ \mu\text{M}$) in KPi (50 mM) pH 7 plus glycerol (20%), KCl (200 mM), and DDM (0.04%). Fluorescence was measured in a total volume of $800\ \mu\text{L}$ under constant stirring at $25\ ^\circ\text{C}$ on a Fluorolog-3 spectrophotometer (Jobin Yvon, settings: excitation wavelength of 409 nm (slit 1 nm), emission wavelength of 540 nm (slit 5 nm), and data points were averaged from measurements of 20 s). Nucleotides to chase the

TNP-ATP were added via a Hamilton syringe pump (Harvard apparatus) in steps of $4.5\ \mu\text{L}$ ATP (2 mM) and for the ATP analogues (0.14 mM) using stock solutions of ATP (357 mM) and for the ATP analogues (25 mM), both dissolved in KPi (50 mM) pH 7) and a mixing time of 15 s. Titration of protein solution with KPi (50 mM) pH 7 were performed to correct for dilution and bleaching during the measurements.

Protein and DNA Constructs. The following ABC transporters were used: OpuA,²⁸ OpuA Δ SBD,²⁹ GlnPQ,³⁰ Sav1866,³¹ and the soluble nucleotide-binding domain (GlcV) of the ABC transporter GlcSTUV.³² The following membrane proteins were used as controls (non-ABC transporters): LacS (C320A/A635C),³³ LacY,³⁴ IIC,³⁵ and RibU.³⁶ The Sav1866 gene construct was cloned into the N-Lic vector pNZnLIC as described by Geertsema et al.³⁷ The genes for GlcV and LacY were expressed in *E. coli*, and all other proteins were produced in *L. lactis* as described in the listed references. GlcV was obtained from M. Pretz and C. van der Does (University Groningen, The Netherlands). Actin (from bovine muscle, A3653), myosin (from rabbit muscle, M1636), and protein kinase A (from bovine heart, P5511) were purchased from Sigma Aldrich.

Profiling with ATP Analogues. Isolation of membrane vesicles and purification of the proteins was done as described.³⁸ Membrane vesicles were prepared in KPi (50 mM) pH 7 at a concentration of ca. 20 mg/mL, unless indicated otherwise; for protein purifications, the membrane vesicles were diluted to 5 mg/mL in KPi (50 mM) pH 7, KCl (200 mM) plus glycerol (20%) and, subsequently, solubilized with DDM (0.5%); purified protein was obtained in KPi (50 mM) pH 7, KCl (200 mM), glycerol (20%), and DDM (0.05%) plus imidazole (200 mM). GlcV was purified in Na-MES (20 mM) pH 6.5 plus NaCl (100 mM) as described by Pretz and colleagues³⁹ and stored in aliquots at $-20\ ^\circ\text{C}$. For profiling with the ATP analogues, protein mixtures were incubated with streptactin column material (Streptactin Sepharose from IBA, binding capacity 300 nmol/mL) in the presence of the ATP analogue, using Biospin Poly-Prep columns (volume 1.2 mL, Biorad). The mixture was incubated for at least 1 h at $4\ ^\circ\text{C}$ (under continuous mixing), before washing and elution of the proteins bound to the column material. The column material was washed in general, with 4 column volumes, prior to elution of the bound proteins with 1 column volume of $2\times$ SDS loading buffer, which is composed of Tris-HCl (100 mM) pH 6 plus glycerol (20%), bromophenol blue

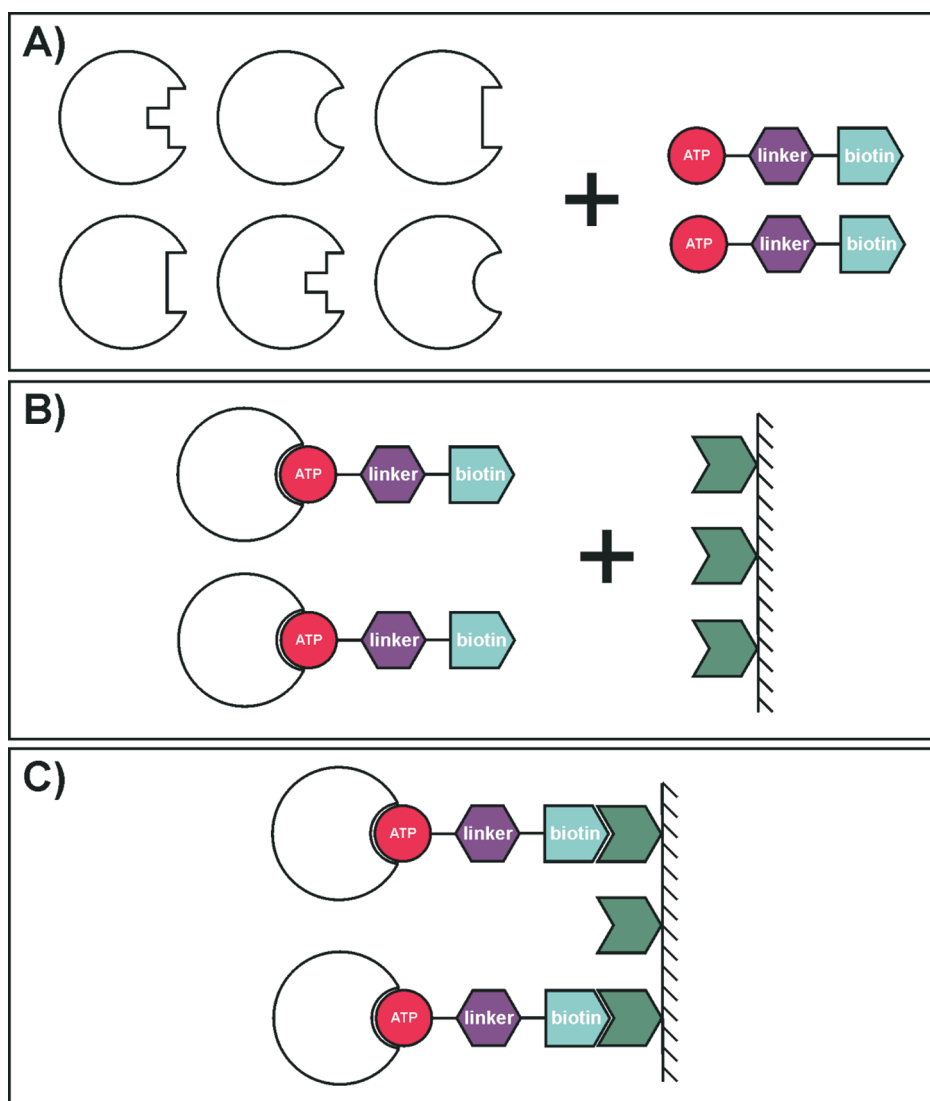


Figure 2. Schematic representation of activity based profiling using an ATP analogue as a probe. Panel A: The ATP (reactive group) moiety of the probe binds specifically to nucleotide-binding proteins within a complex sample. Panel B: The biotin (reporter group) moiety of the probe is used for enrichment of the proteins on streptactin column material. Panel C: The proteins enriched via this method can be analyzed after elution.

(0.002%), and SDS (4%) plus β -mercaptoethanol (1%). Analysis of the protein samples was done on SDS-PAGE gels (12.5%, stained with Coomassie brilliant blue) or subsequent immunoblotting on polyvinylidene difluoride (PVDF) membrane, using the semidry electroblotting technique (blotting for 35 min at 80 mA per blot). Immunodetection was done with an antibody (Amersham Pharmacia Biotech) against the His-tag of the various proteins. The signals were imaged with a CCD camera (Fujifilm, Las-3000 imaging system), using the Western light kit (Tropix Inc.), and quantification of the signals from the SDS-PAGE gels and immunoblots was done with the *AIDA* image analyzer software (version 4.15).

Analytical RP-HPLC. Analytical RP-HPLC was performed using a polystyrene/divenyl benzene column (Source 5RPC ST 4.6/150) connected to an Äkta-purifier system. Two buffers were used for the separation: Buffer A2, triethyl ammonium acetate (TEAA, 100 mM) pH 7.0, and Buffer B2, acetonitrile plus TEAA (100 mM) pH 7.0. The settings for the separations were as follows: 200 μ L loop, flow rate 1 mL/min, gradient: 5 min 17%

buffer B2, 10 min gradient 17–20% buffer B2, 5 min 90% buffer B2, 5 min 0% B.

RESULTS AND DISCUSSION

Design of the ATP Analogues. (+)-Biotin-hex-acyl-ATP (BHacATP) has been used for activity-based profiling of protein kinases.⁴⁰ Protein kinases have a conserved lysine in the binding pocket, i.e., near the phosphates of the nucleotide.^{41,42} The electrophilic acyl-phosphate bond of the analogue couples with the ϵ -amine from this lysine, connecting the biotinylated linker to the protein and freeing it from the nucleotide. Using this analogue, 136 proteins, mostly ATP phosphohydrolases, (protein) kinases, and several heat shock proteins, were identified in lysates of breast cancer cells.⁴⁰ However, this probe is not suitable for ABC proteins, because the space for the hexyl-linker with the biotin moiety would be too limited. On the basis of the structures of ABC transporters, relatively large modifications are likely to be tolerated at the 2'- and 3'-OH of the ribose (Figure 1). The

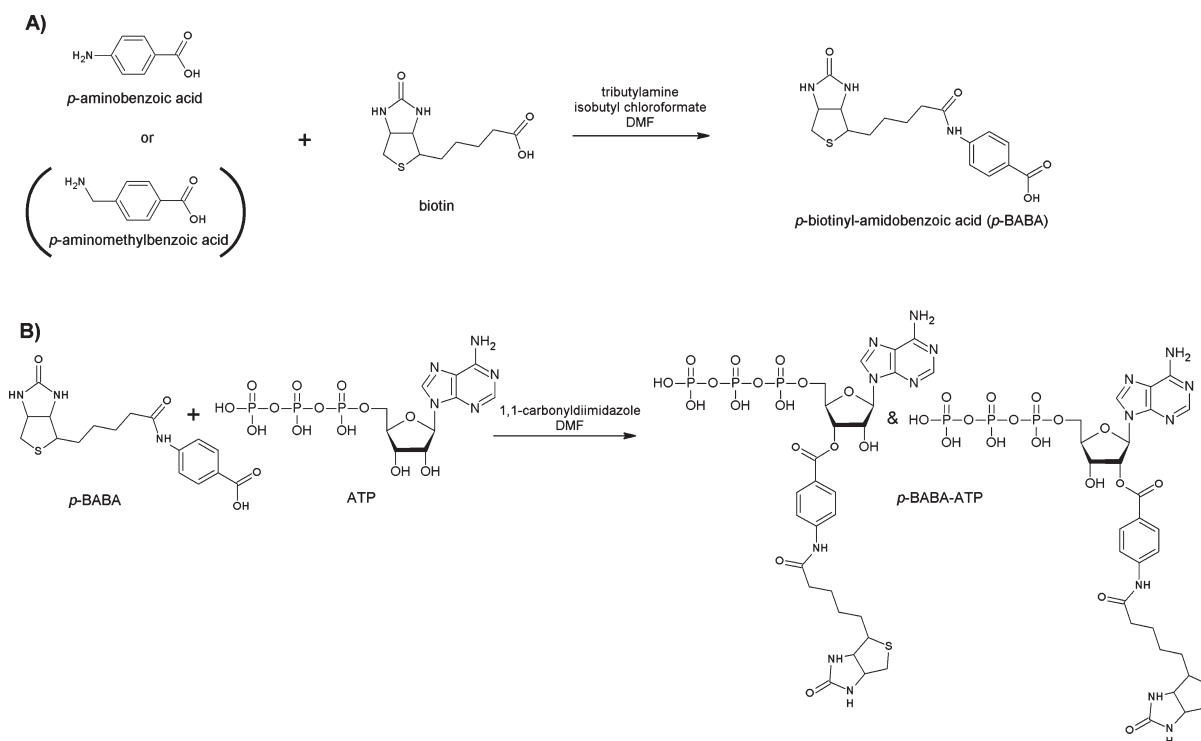


Figure 3. Chemical structures and reaction schemes for the synthesis of the two ATP analogues. Panel A: Synthesis of the biotinylated linkers *p*-biotinyl-amidobenzoic acid (*p*-BABA) and *p*-biotinyl-amidomethylbenzoic acid (*p*-BAMBA). Panel B: Synthesis of *p*-biotinyl-amidobenzoic acid-ATP, shown as two isoforms, from the biotinylated linker and ATP.

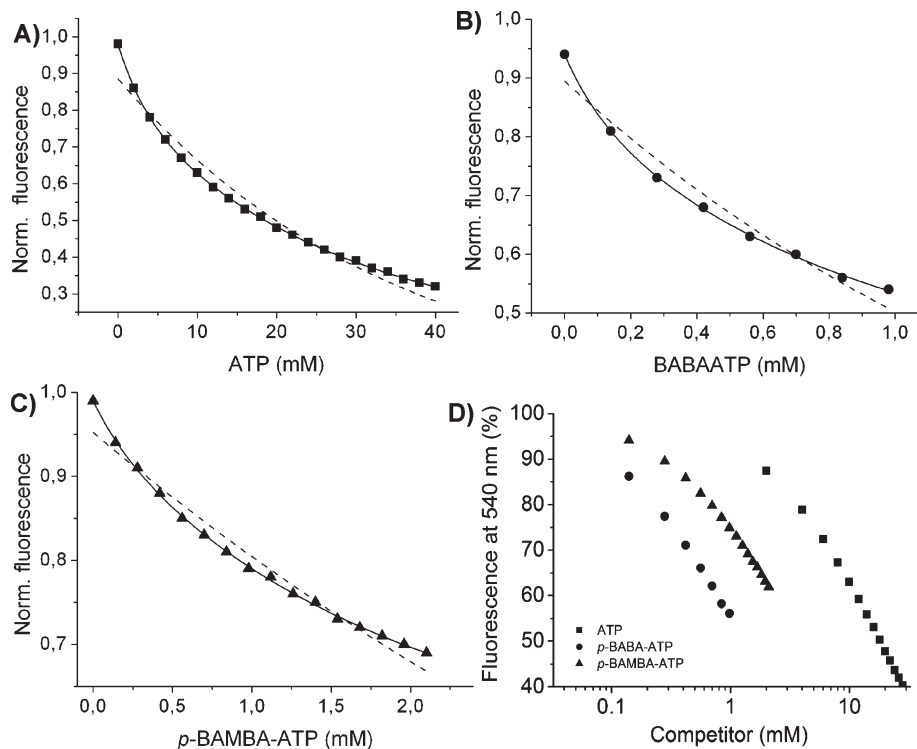


Figure 4. Nucleotide-binding properties of the ATP analogues *p*-BABA-ATP and *p*-BAMBA-ATP. Binding of ATP or the ATP analogues was measured by competition with the TNP-ATP bound to the purified ABC transporter OpuA. Panels A, B, and C show the fluorescence decay upon addition of ATP, *p*-BABA-ATP, and *p*-BAMBA-ATP, respectively, and fitting of the results with single (dashed lines) and double (solid lines) exponential decay fits. Panel D compiles the results collectively on a logarithmic scale.

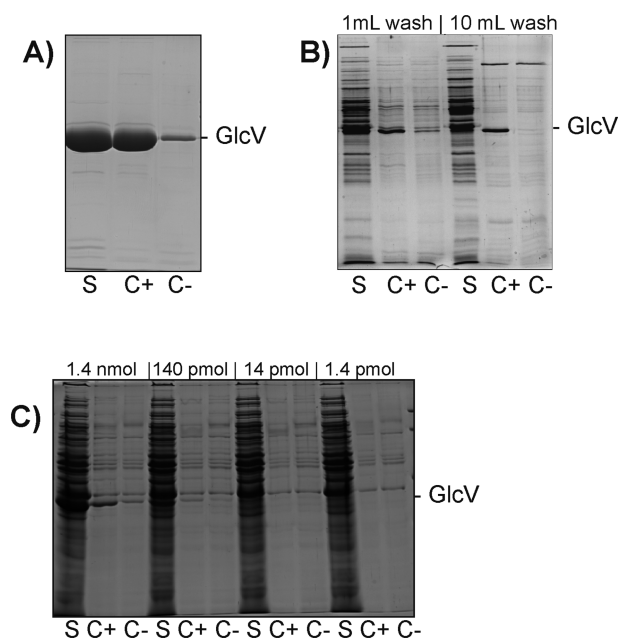


Figure 5. SDS-PAA gels of protein binding to streptactin columns (30 nmol binding sites) in the presence or absence of the ATP analogue *p*-BABA-ATP (30 nmol), using the nucleotide-binding protein GlcV of a glucose ABC transporter from *S. solfataricus* as test sample. Panel A shows the binding of GlcV in the presence or absence of *p*-BABA-ATP as a purified fraction of GlcV (3.4 nmol). Panel B shows the binding of purified GlcV (0.6 nmol) mixed in a *L. lactis* crude cell lysate (0.2 mg) after washing of the column fraction with 1 or 10 mL of washing buffer using 50 mM Na-MES pH 7. Panel C shows the profiling of GlcV present in *L. lactis* crude cell lysates (0.2 mg) at concentrations of 1.4 nmol to 140 pmol GlcV, corresponding to about 27–0.027% of GlcV protein in the lysate using 50 mM KP, pH 7 as buffer. Annotations are as follows: start material (S) and fractions eluted from the column (C); (+) means that proteins were incubated with the column material in the presence of *p*-BABA-ATP and (–) in the absence of ATP analogue. Equal volumes of each fraction were loaded on the gel.

structure of the nucleotide binding protein HlyB indicates that certain modifications may affect the interaction between the ribose of the nucleotide and a glutamine residue in the C-loop of the ABC proteins.⁴³ We thus designed two ATP analogues with a linker coupled to the ribose to keep the biotin group accessible for binding to a chromatography resin. We introduced an aromatic group in the linker, as previous studies had shown that an aromatic group like trinitrophenol linked to ATP (TNP-ATP) binds to ABC proteins with much higher affinity than genuine ATP.^{19,44,45} In fact, ABC transporters have been reported to bind ATP with K_D values in the submillimolar to low millimolar range, which is too low for efficient profiling of the proteins. Guided by these observations, the aromatic ring-structure was used as the basis for the design of the linkers to couple the biotin moiety to ATP. For the activity-based protein profiling with these probes (as summarized in Figure 2), the ATP moiety is the bait to enrich for the ABC proteins, and the biotin moiety is the reporter tag for enrichment.

Synthesis of the ATP Analogues. The general synthetic approach was designed and optimized for biotinyl-amidobenzoic acid-ATP (*p*-BABA-ATP). The synthesis of biotinyl-amidobenzoic acid (Figure 3A) was achieved as described previously for biotinylated amino acid precursors, using isobutyl chloroformate to activate the biotin prior to reaction with the amine of the linker moiety.²⁶

A second linker, that is, 4-aminomethylbenzoic acid, was used to synthesize 4-biotinylamidomethylbenzoic acid (*p*-BAMBA) (Figure 3A). The presence of an additional methylene group compared to *p*-BABA resulted in a significant decrease in the solubility of the biotinylated linker in DMF. The coupling of the biotinylated linker to adenosine triphosphate (ATP) was based on a method described for 3'-*O*-(4-benzoyl)benzoyl-ATP.²⁷ This involved the activation of the acid group from biotin with carbonyldiimidazole,⁴⁶ which subsequently reacted with a hydroxyl group on the ribose ring of ATP to form an ester linkage (Figure 3B).

The ratio between ATP and *p*-BABA was varied from 1:8 to 2:1. With an 8-fold excess of *p*-BABA, hardly any *p*-BABA-ATP was formed (data not shown). The optimal yield of *p*-BABA-ATP was found using equimolar amounts of ATP and *p*-BABA as judged by reversed-phase HPLC analysis (Supporting Information Figure S5A-B). However, ESI MS analysis showed only a single peak at m/z 851. This can be explained by the formation of two isomeric products, resulting from the coupling of the biotinylated linker to the 2'- and 3'-OH group of the ribose ring of ATP.

The reaction time was varied from 1 to 25 h (Supporting Information Figure S5B) with the highest yield after 25 h. Notably, the *p*-BABA-ATP isomer of the first peak was formed first and the other isomer only after longer conversion times (>1 h).

Two purification steps were performed to obtain the pure ATP derivatives: after preparative RP-HPLC (pRP-HPLC) purification, the ATP-derivative containing fractions were pooled and further purified on a strong anion exchange resin (monoQ sepharose). *p*-BABA-ATP and *p*-BAMBA-ATP eluted at 1 M TEAA pH 7 and the ESI-MS analysis of the pooled elution fractions (elution fractions 1–3) showed a clean signal for the ATP analogue (Supporting Information Figure S5C-G).

Structural Properties. The ESI-MS spectra of the product proved that the coupling of *p*-BABA to ATP was successful but did not establish connectivity of the product, that is, the position of the coupling. Although literature reports suggest the present method to result at the 2'-OH or 3'-OH position of the ribose ring,²⁷ in principle, also, coupling to the γ -phosphate or the amine group of the adenine ring can occur. NMR analysis was complicated as a result of the formation of the two isomers (Supporting Information Figure S4). However, the appearance of new signals in the ¹H NMR spectra between 5 and 6 ppm with the expected multiplicity corresponds to what was reported for the ribose modified ATP-analogue BzATP,²⁷ indicating that the linker is coupled to the ribose hydroxy groups. Measurements with ¹³C NMR (¹³C NMR and HSQC) were limited by the low solubility of the ATP analogue. The spectra did not improve enough at higher temperatures or longer measurement times (up to 1 week).

A variety of other methods were used to demonstrate the coupling of the biotinylated linker to the hydroxyl groups of the ribose ring of ATP. Measurements of *p*-BABA-ATP and ATP with ³¹P NMR showed equal spectra (both with shifts at 39.2 ppm (t) and 51.2 ppm (dd)), which excludes coupling of the *p*-BABA to the γ -phosphate of ATP. Partial hydrolysis and detection by ESI-MS (and MSMS) of *p*-BABA-ATP was used to distinguish between coupling of the biotinylated linker to the amine group of the adenine ring or the hydroxyl groups of the ribose ring. The ESI-MS spectrum of the ATP analogue after hydrolysis with sodium carbonate in methanol did show

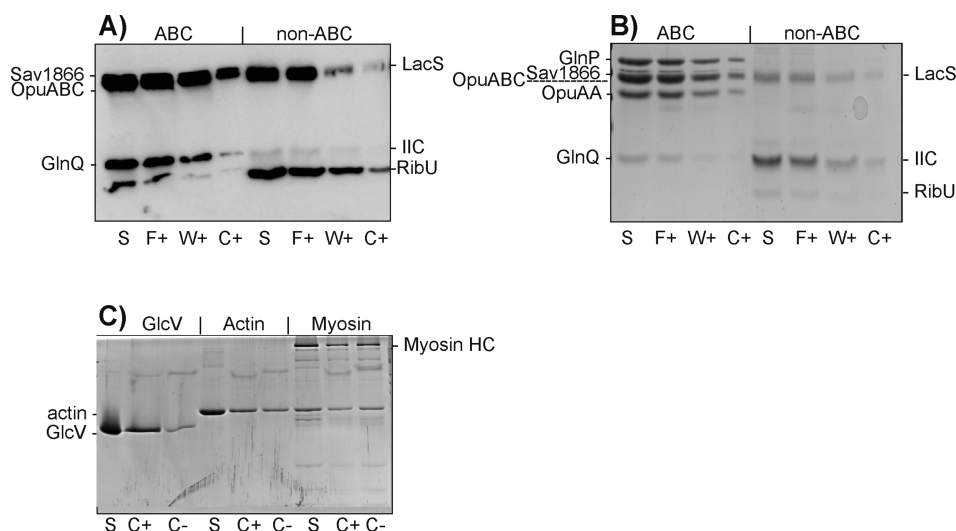


Figure 6. Immunoblot (panel A) and SDS-PAGE gel (panels B and C) monitoring the binding of ABC transporters, non-ABC transporters, and other nucleotide-binding proteins from mixtures of purified proteins [15–30 μg purified protein (panel A and B) and 80 μg protein (panel C)] to streptactin [15 nmol (panel A and B) and 30 nmol (panel C) binding sites] in the presence of *p*-BABA-ATP [15 nmol (panel A and B) and 30 nmol (panel C)]. 50 mM KP_i, pH 7 plus 200 mM KCl was used as buffer for these experiments, supplemented with 0.04% DDM for the samples with purified membrane proteins. The following ABC transporter proteins: OpuA, GlnPQ, and Sav1866 were used; RibU, LacS, and the IIC domain of the mannitol-PTS (panel A and B) served as controls, as these proteins do not contain a nucleotide-binding site; actin and myosin (myosin heavy chains (myosin HC) binds the ATP) (panel C) were used as a second set of controls as these are non-ABC type nucleotide-binding proteins. Annotations are as follows: start material (S), flowthrough (F), wash fraction (W), and fractions eluted from the column (C), (+) means that proteins were incubated with the column material in the presence of *p*-BABA-ATP and (–) in the absence of ATP analogue. Equal volumes of each fraction were loaded on the gel.

transesterification of *p*-BABA-ATP (Supporting Information Figure S6) and the methyl ester of *p*-BABA could be detected. Reaction of the amide bonds under these conditions is highly unlikely, as it is illustrated that the amide bond between the biotin and linker moiety remained intact under these conditions. In combination, these experiments demonstrate that *p*-BABA is indeed attached to the 2'/3'-OH group via an ester linkage.

Nucleotide-Binding Properties. A competition assay was used to determine the binding properties of *p*-BABA-ATP and *p*-BAMBA-ATP relative to that of ATP. The purified ABC transporter OpuA from *Lactococcus lactis*⁴⁷ was used as a model protein to assess the relative binding affinities. The nucleotide binding affinity of OpuA for ATP is in the millimolar range and cannot be probed directly. The fluorescent ATP analogue trinitrophenyl-adenosine triphosphate (TNP-ATP) binds to OpuA with micromolar affinity, and the relative affinity of ATP or other analogues can be accessed via competitive nucleotide-binding studies⁴⁸ (Figure 4). Figure 4A,B,C shows the decrease in TNP-ATP fluorescence with increasing concentration of ATP, *p*-BABA-ATP, and *p*-BAMBA-ATP, respectively. The data were fitted with single- and double-exponential decay functions, and only the latter yielded excellent fits. The data are indicative of low- and high-affinity binding of TNP-ATP, which most likely reflects the open (low-affinity) and closed (high-affinity) conformation of the nucleotide-binding domains. The data and interpretation are consistent with observations on the soluble nucleotide-binding protein OpuAA from *B. subtilis*: here, the low- and high-affinity binding correspond to the monomeric and dimeric nucleotide-binding domains.¹⁹ In the concentration range used, the high-affinity component of TNP-ATP binding could not be fully chased with ATP, *p*-BABA-ATP, or *p*-BAMBA-ATP; for economic reasons, we did not titrate at higher concentrations as it would have taken an impractical amount of

synthesized ATP (analogue) to chase all TNP-ATP. Despite the complex biphasic kinetics, the data clearly show that both *p*-BABA-ATP and *p*-BAMBA-ATP were at least 10-fold more efficient in competing with TNP-ATP from the binding pocket of OpuA than ATP; *p*-BABA-ATP displayed the highest affinity (Figure 4D). These measurements show that the linker does improve the binding affinity of the nucleotide analogues to the ABC transporter OpuA.

Binding of Nucleotide-Binding Proteins. Binding of the proteins via the ATP analogues was confirmed by SDS-PAGE analysis using the soluble nucleotide-binding domain (GlcV) of the glucose ABC transporter from *Sulfolobus solfataricus* (with a nanomolar affinity for ATP³⁹). GlcV bound efficiently to streptactin column material in the presence of *p*-BABA-ATP as can be seen in Figure 5A. Spiking of GlcV to a crude cell free extract of *L. lactis* (0.2 mg total protein) at a protein concentration of 3 μM GlcV still yielded a highly significant binding in the presence of *p*-BABA-ATP (Figure 5B). Quantification of the signals on the SDS-PAGE gel showed that about 41% of the GlcV was bound to the column in the presence of *p*-BABA-ATP, which compares to 6% (unspecific binding) in the absence of the ATP analogue. Further dilution of GlcV into the crude cell free extract showed that specific binding could still be detected until a concentration of 0.7 μM (140 pmol) of GlcV (Figure 5C).

Next, mixtures of three purified ABC transporters (OpuA, GlnPQ, and Sav1866) and three non-ABC transporters (LacS, RibU, and IIC) were compared (Figure 6A,B), where the membrane proteins lacking a nucleotide-binding site (non-ABC transporters) are used as controls for the levels of nonspecific binding. Sav1866 and OpuA showed clear binding. The fact that OpuAA was detected by immunoblotting indicated that the whole complex of OpuA was bound since the His-tag is on OpuABC subunit and *p*-BABA-ATP is binding to the OpuAA

subunit. In the case of GlnPQ, the His-tag is on the ATPase subunit (GlnQ), but no binding of GlnQ was detected. However, GlnP (the transmembrane domain-substrate binding protein) was detected on SDS-PAGE gels, most likely reflecting aspecific binding. LacS and IIC did not significantly bind to the streptactin column. Experiments using detergent-solubilized membrane vesicles with overexpressed proteins yielded similar results (data not shown). The results show that ABC transporters can be enriched specifically with the ATP analogues, but the presence of residual protein in the flowthrough and wash fractions indicates that a further improvement in binding affinity would be desirable. We also assessed the binding of other types of nucleotide-binding proteins, namely, actin, myosin, and protein kinase A, for which the probes were not designed. No specific binding was observed for any of these proteins (Figure 6C; data for protein kinase A is not shown), confirming the specificity of the probes for ABC-type nucleotide-binding proteins.

CONCLUSION

Two ATP analogues with biotinylated linkers coupled to the hydroxyl groups of the ribose ring of ATP were synthesized successfully, namely, *p*-biotinyl amidobenzoic acid-ATP (*p*-BABA-ATP) and *p*-biotinyl aminomethylbenzoic acid-ATP (*p*-BAMBA-ATP). The coupling of biotin to the linker was demonstrated by ¹H and ¹³C NMR, and the correct coupling of the biotinylated linker to the ATP was deduced from ESI-MS/MSMS analyses of partial digests of the ATP analogues and ³¹P NMR. Ligand-binding experiments showed that the two ATP analogues bind to the ABC transporter OpuA with at least 1 order of magnitude higher affinity than genuine ATP. The presence of the biotin moiety on the analogues was exploited for the enrichment and profiling of nucleotide-binding proteins. Relatively specific binding was demonstrated for several ABC transporters.

ASSOCIATED CONTENT

S Supporting Information. NMR spectra (Figure S1–4), RP-HPLC/MS spectra (Figure S5–6), and absorbance analyses (Figure S7) of the synthesis steps. This material is available free of charge via the Internet at <http://pubs.acs.org>.

AUTHOR INFORMATION

Corresponding Author

*Bert Poolman, Nijenborgh 4, 9747AG, Groningen, The Netherlands. Tel: +31 50 3634190. Fax: +31 50 3634195. E-mail: b.poolman@rug.nl.

ACKNOWLEDGMENT

We would like to thank Hjalmar Permentier for his help with the ESI-MS/MSMS measurements, and Ruud Scheek and Renee Otten for their help with the NMR measurements. We would like to thank the following people for providing purified proteins or membrane vesicles: Monika Pretz and Chris van der Does (purified GlcV), Gea Schuurman-Wolters (GlnPQ, IIC, Sav1866, LacY), Siva Ramadurai (LacS), Josy ter Beek (RibU), Guus Erkens (soluble cell free extracts) and Faizah Fulyani (soluble cell free extracts). We would like to thank Wim Huibers and Fabrizia Fusetti for their help with the LC-MS measurements. This work was supported by grants from The Netherlands Organisation for Scientific research (NWO, Chemical Sciences

Top Subsidy to BP; grant number 700-56-302 and The Netherlands Proteomics Centre (NPC).

REFERENCES

- (1) Heal, W. P., Wickramasinghe, S. R., and Tate, E. W. (2008) Activity based chemical proteomics: profiling proteases as drug targets. *Curr. Drug Discovery Technol.* 5, 200–212.
- (2) Kolb, H. C., Finn, M. G., and Sharpless, K. B. (2001) Click chemistry: diverse chemical function from a few good reactions. *Angew. Chem., Int. Ed. Engl.* 40, 2004–2021.
- (3) Speers, A. E., Adam, G. C., and Cravatt, B. F. (2003) Activity-based protein profiling in vivo using a copper(i)-catalyzed azide-alkyne [3 + 2] cycloaddition. *J. Am. Chem. Soc.* 125, 4686–4687.
- (4) Speers, A. E., and Cravatt, B. F. (2004) Profiling enzyme activities in vivo using click chemistry methods. *Chem. Biol.* 11, 535–546.
- (5) Barglow, K. T., and Cravatt, B. F. (2007) Activity-based protein profiling for the functional annotation of enzymes. *Nat. Methods* 4, 822–827.
- (6) Cravatt, B. F., Wright, A. T., and Kozarich, J. W. (2008) Activity-based protein profiling: from enzyme chemistry to proteomic chemistry. *Annu. Rev. Biochem.* 77, 383–414.
- (7) Evans, M. J., and Cravatt, B. F. (2006) Mechanism-based profiling of enzyme families. *Chem. Rev.* 106, 3279–3301.
- (8) Hagenstein, M. C., and Sewald, N. (2006) Chemical tools for activity-based proteomics. *J. Biotechnol.* 124, 56–73.
- (9) Schmidinger, H., Hermetter, A., and Birner-Gruenberger, R. (2006) Activity-based proteomics: enzymatic activity profiling in complex proteomes. *Amino Acids* 30, 333–350.
- (10) Sieber, S. A., and Cravatt, B. F. (2006) Analytical platforms for activity-based protein profiling—exploiting the versatility of chemistry for functional proteomics. *Chem. Commun. (Camb.)* 2311–2319.
- (11) Uttamchandani, M., Li, J., Sun, H., and Yao, S. Q. (2008) Activity-based protein profiling: new developments and directions in functional proteomics. *ChemBioChem* 9, 667–675.
- (12) Bagshaw, C. R. (2001) ATP analogues at a glance. *J. Cell Sci.* 114, 459–460.
- (13) Cremo, C. R. (2003) Fluorescent nucleotides: Synthesis and characterization. *Biophotonics, Part A* 360, 128–177.
- (14) Jameson, D. M., and Eccleston, J. F. (1997) Fluorescent nucleotide analogs: Synthesis and applications. *Fluoresc. Spectrosc.* 278, 363–390.
- (15) Yount, R. G. (1975) ATP analogs. *Adv. Enzymol. Relat. Areas Mol. Biol.* 43, 1–56.
- (16) Davidson, A. L., Dassa, E., Orelle, C., and Chen, J. (2008) Structure, function, and evolution of bacterial ATP-binding cassette systems. *Microbiol. Mol. Biol. Rev.* 72, 317–64, table.
- (17) Dean, M. (2005) The genetics of ATP-binding cassette transporters. *Methods Enzymol.* 400, 409–429.
- (18) al Shawi, M. K., Urbatsch, I. L., and Senior, A. E. (1994) Covalent inhibitors of P-glycoprotein ATPase activity. *J. Biol. Chem.* 269, 8986–8992.
- (19) Horn, C., Bremer, E., and Schmitt, L. (2003) Nucleotide dependent monomer/dimer equilibrium of OpuAA, the nucleotide-binding protein of the osmotically regulated ABC transporter OpuA from *Bacillus subtilis*. *J. Mol. Biol.* 334, 403–419.
- (20) Liu, R. H., and Sharom, F. J. (1997) Fluorescence studies on the nucleotide binding domains of the P-glycoprotein multidrug transporter. *Biochemistry* 36, 2836–2843.
- (21) Orelle, C., Ayvaz, T., Everly, R. M., Klug, C. S., and Davidson, A. L. (2008) Both maltose-binding protein and ATP are required for nucleotide-binding domain closure in the intact maltose ABC transporter. *Proc. Natl. Acad. Sci. U. S. A.* 105, 12837–12842.
- (22) Shapiro, A. B., and Ling, V. (1995) Reconstitution of drug transport by purified P-glycoprotein. *J. Biol. Chem.* 270, 16167–16175.
- (23) Verdon, G., Albers, S. V., Dijkstra, B. W., Driessen, A. J., and Thunnissen, A. M. (2003) Crystal structures of the ATPase subunit of

the glucose ABC transporter from *Sulfolobus solfataricus*: nucleotide-free and nucleotide-bound conformations. *J. Mol. Biol.* 330, 343–358.

(24) Morbach, S., Tebbe, S., and Schneider, E. (1993) The ATP-binding cassette (ABC) transporter for maltose/maltodextrins of *Salmonella typhimurium*. Characterization of the ATPase activity associated with the purified MalK subunit. *J. Biol. Chem.* 268, 18617–18621.

(25) Sauna, Z. E., Kim, I. W., Nandigama, K., Kopp, S., Chiba, P., and Ambudkar, S. V. (2007) Catalytic cycle of ATP hydrolysis by P-glycoprotein: evidence for formation of the E.S reaction intermediate with ATP- γ -S, a nonhydrolyzable analogue of ATP. *Biochemistry* 46, 13787–13799.

(26) Skander, M., Humbert, N., Collot, J., Gradinaru, J., Klein, G., Loosli, A., Sauser, J., Zocchi, A., Gilardoni, F., and Ward, T. R. (2004) Artificial metalloenzymes: (Strept)avidin as host for enantioselective hydrogenation by achiral biotinylated rhodium-diphosphine complexes. *J. Am. Chem. Soc.* 126, 14411–14418.

(27) Williams, N., and Coleman, P. S. (1982) Exploring the adenine-nucleotide binding-sites on mitochondrial F1-ATPase with a new photoaffinity probe, 3'-O-(4-benzoyl)benzoyl adenosine 5'-triphosphate. *J. Biol. Chem.* 257, 2834–2841.

(28) van der Heide, T., and Poolman, B. (2000) Osmoregulated ABC-transport system of *Lactococcus lactis* senses water stress via changes in the physical state of the membrane. *Proc. Natl. Acad. Sci. U. S. A.* 97, 7102–7106.

(29) Biemans-Oldehinkel, E., and Poolman, B. (2003) On the role of the two extracytoplasmic substrate-binding domains in the ABC transporter OpuA. *EMBO J.* 22, 5983–5993.

(30) Schuurman-Wolters, G. K., and Poolman, B. (2005) Substrate specificity and ionic regulation of GlnPQ from *Lactococcus lactis*. An ATP-binding cassette transporter with four extracytoplasmic substrate-binding domains. *J. Biol. Chem.* 280, 23785–23790.

(31) Dawson, R. J., and Locher, K. P. (2006) Structure of a bacterial multidrug ABC transporter. *Nature* 443, 180–185.

(32) Verdon, G., Albers, S. V., Dijkstra, B. W., Driessen, A. J., and Thunnissen, A. M. (2002) Purification, crystallization and preliminary X-ray diffraction analysis of an archaeal ABC-ATPase. *Acta Crystallogr., Sect. D: Biol. Crystallogr.* 58, 362–365.

(33) Doeven, M. K., Folgering, J. H., Krasnikov, V., Geertsma, E. R., van den Bogaart, G., and Poolman, B. (2005) Distribution, lateral mobility and function of membrane proteins incorporated into giant unilamellar vesicles. *Biophys. J.* 88, 1134–1142.

(34) Teather, R. M., Bramhall, J., Riede, I., Wright, J. K., Furst, M., Aichele, G., Wilhelm, U., and Overath, P. (1980) Lactose carrier protein of *Escherichia coli*. Structure and expression of plasmids carrying the Y gene of the lac operon. *Eur. J. Biochem.* 108, 223–231.

(35) Boer, H., Hoeve-Duurkens, R. H., Schuurman-Wolters, G. K., Dijkstra, A., and Robillard, G. T. (1994) Expression, purification, and kinetic characterization of the mannitol transport domain of the phosphoenolpyruvate-dependent mannitol phosphotransferase system of *Escherichia coli*. Kinetic evidence that the *E. coli* mannitol transport protein is a functional dimer. *J. Biol. Chem.* 269, 17863–17871.

(36) Burgess, C. M., Slotboom, D. J., Geertsma, E. R., Duurkens, R. H., Poolman, B., and van Sinderen, D. (2006) The riboflavin transporter RibU in *Lactococcus lactis*: molecular characterization of gene expression and the transport mechanism. *J. Bacteriol.* 188, 2752–2760.

(37) Geertsma, E. R., and Poolman, B. (2007) High-throughput cloning and expression in recalcitrant bacteria. *Nat. Methods* 4, 705–707.

(38) Biemans-Oldehinkel, E., Mahmood, N. A., and Poolman, B. (2006) A sensor for intracellular ionic strength. *Proc. Natl. Acad. Sci. U. S. A.* 103, 10624–10629.

(39) Pretz, M. G., Albers, S. V., Schuurman-Wolters, G., Tampe, R., Driessen, A. J. M., and van der Does, C. (2006) Thermodynamics of the ATPase cycle of GlcV, the nucleotide-binding domain of the glucose ABC transporter of *Sulfolobus solfataricus*. *Biochemistry* 45, 15056–15067.

(40) Patricelli, M. P., Szardenings, A. K., Liyanage, M., Nomanbhoy, T. K., Wu, M., Weissig, H., Aban, A., Chun, D., Tanner, S., and Kozarich, J. W. (2007) Functional interrogation of the kinome using nucleotide acyl phosphates. *Biochemistry* 46, 350–358.

(41) Zheng, J., Knighton, D. R., Ten Eyck, L. F., Karlsson, R., Xuong, N., Taylor, S. S., and Sowadski, J. M. (1993) Crystal structure of the catalytic subunit of cAMP-dependent protein kinase complexed with MgATP and peptide inhibitor. *Biochemistry* 32, 2154–2161.

(42) Hanks, S. K., and Hunter, T. (1995) Protein kinases 6. The eukaryotic protein kinase superfamily: kinase (catalytic) domain structure and classification. *FASEB J.* 9, 576–596.

(43) Oswald, C., Holland, I. B., and Schmitt, L. (2006) The motor domains of ABC-transporters. What can structures tell us? *Naunyn-Schmiedeberg's Arch. Pharmacol.* 372, 385–399.

(44) Qu, Q., Russell, P. L., and Sharom, F. J. (2003) Stoichiometry and affinity of nucleotide binding to P-glycoprotein during the catalytic cycle. *Biochemistry* 42, 1170–1177.

(45) Oswald, C., Jenewein, S., Smits, S. H., Holland, I. B., and Schmitt, L. (2008) Water-mediated protein-fluorophore interactions modulate the affinity of an ABC-ATPase/TNP-ADP complex. *J. Struct. Biol.* 162, 85–93.

(46) Gottikh, B. P., Krayevsky, A. A., Tarusova, N. B., Purygin, P. P., and Tsilevich, T. L. (1970) The general synthetic route to amino acid esters of nucleotides and nucleoside-5'-triphosphates and some properties of these compounds. *Tetrahedron* 26, 4419–4433.

(47) Patzlaff, J. S., van der Heide, T., and Poolman, B. (2003) The ATP/substrate stoichiometry of the ATP-binding cassette (ABC) transporter OpuA. *J. Biol. Chem.* 278, 29546–29551.

(48) Wolters, J. C., Berntsson, R. P., Gul, N., Karasawa, A., Thunnissen, A. M., Slotboom, D. J., and Poolman, B. (2010) Ligand binding and crystal structures of the substrate-binding domain of the ABC transporter OpuA. *PLoS One* 5, e10361.

(49) Smith, P. C., Karpowich, N., Millen, L., Moody, J. E., Rosen, J., Thomas, P. J., and Hunt, J. F. (2002) ATP binding to the motor domain from an ABC transporter drives formation of a nucleotide sandwich dimer. *Mol. Cell* 10, 139–149.